Applications of Mickens Finite Differences to Several Related Boundary Value Problems

by Ron Buckmire *

buckmire@oxy.edu
Mathematics Department
Occidental College
1600 Campus Road
Los Angeles, CA 90041-3338, U.S.A.

April 7, 2005

The initial discovery and implementation by the author of a particular kind of nonstandard finite difference (NSFD) scheme called a "Mickens finite difference" (MFD) for approximating the radial derivatives of the Laplacian in cylindrical coordinates is reviewed. The development of a similar scheme for the spherical coordinates case is also recounted. Examples of application of the schemes to several related (singular and nonsingular, linear and nonlinear) boundary value problems are given. Examples of applying Buckmire's MFD scheme to the bifurcatory, nonlinear eigenvalue problems of Bratu and Gel'fand are also presented. The results support the utility and versatility of MFD schemes for boundary value problems with singularities or bifurcations.

Keywords: NSFD, MFD, Bratu problem, Gelfand problem, nonstandard finite differences, Mickens finite difference, bifurcation, singular, nonlinear, eigenvalue

*The author is Associate Professor and Chairperson of Mathematics at Occidental College.

1 Introduction

In this paper a review of the discovery, development and various implementations by the author of a specific Mickens finite difference (MFD) shall be presented. Application of this MFD leads to nonstandard finite difference (NSFD) schemes which can be used to efficiently approximate solutions to various boundary value problems. Boundary value problems associated with Bratu, Gel'fand and others are considered. The MFD schemes given here produce new and different ways to discretize the Laplacian operator $r^p \dfrac{d}{dr}$, where $p = 1$ is the cylindrical case and $p = 2$ is the spherical case. They are examples of the kinds of numerical methods Professor Ronald E. Mickens of Clark Atlanta University has analyzed and popularized for years ([31], [32], [33], et cetera).

In Section 2 of this paper the discovery and development of the Mickens finite difference by the author is recounted. The initial application was to a mixed-type, nonlinear elliptic-hyperbolic partial differential equation with singular boundary conditions found in theoretical aerodynamics. These results have previously appeared in [6], [7] and [8] and are reviewed here.

In Section 3, the application of MFD schemes to two linear singular boundary value problems with known exact solutions which are related to the transonic aerodynamics problem discussed in Section 2 are recounted. These results have appeared in a more detailed fashion in [9].

In Section 4, an MFD scheme is applied to a different nonlinear, singular boundary value problem which is related to the linear, singular boundary value problems of Section 3 and also has known exact multi-valued solutions. These results have appeared in a more detailed fashion in [10].

In Section 5, an MFD scheme is applied to a nonsingular, nonlinear boundary value problem related to the singular, nonlinear boundary value problem of Section 4 which also has known exact multi-valued solutions related to the problem in Section 4. These results have not previously appeared in print.

The paper concludes with discussion about the versatility of Mickens finite differences for application with diverse kinds of boundary value problems and some suggestions for future work.

2 The Buckmire MFD Schemes

The goal of this section of the paper is to provide the background history for the development of the Mickens finite difference which is the main topic of this paper and is discussed further in Section 3 and Section 4. In Buckmire's 1994 thesis [6] this MFD was introduced in order to find particular slender bodies of revolution that possess shock-free flows as specific numerical solutions of a mixed-type, singular boundary value problem. The problem is formulated using transonic small disturbance theory found in [12], [13] and [14], among other sources. Cole & Schwendeman announced the first computation of a fore-aft, symmetric, shock-free transonic slender body in [16]. This work was expanded in [6], which led to the first computation of shock-free, transonic, slender bodies with axisymmetry but without fore-aft symmetry. Basically, the problem involves numerically solving a boundary value problem with an elliptic-hyperbolic partial differential equation (the Kármán-Guderley equation) in cylindrical coordinates, with a singular inner Neumann boundary condition at $r = 0$ and a non-singular outer Dirichlet boundary condition far away from $r = 0$. Namely,

$$(K - (\gamma + 1)\phi_x)\phi_{xx} + \phi_{\tilde{r}\tilde{r}} + \frac{1}{\tilde{r}}\phi_{\tilde{r}} = 0. \tag{1}$$

$$\begin{array}{ll} \phi(x, \tilde{r}) \to S(x) \log \tilde{r} + G(x), & \text{as } \tilde{r} \to 0,\ |x| \leq 1 \\ \phi(x, \tilde{r}) \text{ bounded}, & \text{for } \tilde{r} = 0,\ |x| > 1. \end{array} \tag{2}$$

$$\phi(x, \tilde{r}) \to \frac{\mathcal{D}}{4\pi} \frac{x}{(x^2 + K\tilde{r}^2)^{3/2}}, \qquad \text{as } (x^2 + \tilde{r}^2)^{1/2} \to \infty. \tag{3}$$

In (1),(2) and (3) the variable $\tilde{r}$ is a scaled cylindrical coordinate, K is the transonic similarity parameter, $\mathcal{D}$ is a dipole strength and $\phi(x, \tilde{r})$ is a velocity disturbance potential. Both $S(x)$ and $G(x)$ are bounded functions. The main point of sketching the boundary value problem here is to emphasize that the function $G(x)$ which occurs in (2) needs to be computed very accurately, because the pressure coefficient on the body depends directly on $G'(x)$. It is the pressure coefficient which allows the determinination of whether the body possesses a shock-free flow. Computing it is complicated by the fact that $\phi(x, \tilde{r})$ and $S(x) \log \tilde{r}$ are both becoming singular as $\tilde{r} \to 0$, which is where the boundary condition must be evaluated, and the quantity $G'(x)$ we require is the *derivative* of the difference between these two large quantities. Thus a numerical method was needed to compute the solution $\phi(x, \tilde{r})$ particularly

accurately as $\tilde{r} \to 0$. It was discovered that an exact, nonstandard finite-difference scheme existed for a simpler, related boundary value problem. This discovery was the motivation for adoption of the scheme introduced in [6] and analyzed and discussed in more detail in [7] and [8]. Upon further analysis the author found other nonstandard finite difference schemes which could be derived for slightly different boundary value problems, and then extended this concept to boundary value problems in spherical coordinates. It is these results which were presented in detail in [9] that are summarized below.

2.1 Derivation of the Buckmire MFD scheme

This subsection shall explain the formal derivation of the Buckmire MFD scheme. It is a nonstandard discretization of the Laplacian operator $\mathcal{R}_p = r^p \dfrac{d}{dr}$, where $p = 1$ or $p = 2$. Laplace's equation in cylindrical coordinates is given by

$$\frac{1}{r}(ru_r)_r + u_{\theta\theta} = 0$$

and clearly contains the $\mathcal{R}_1$ operator. Laplace's equation in spherical coordinates is given by

$$\frac{1}{r^2}(r^2u_r)_r + u_{\theta\theta} = 0$$

and clearly contains the $\mathcal{R}_2$ operator. The Kármán-Guderley equation (1) which was the subject of [6] also contains $\mathcal{R}_1$, the radial derivatives of the Laplacian in cylindrical coordinates. The first step in the discretization of the $\mathcal{R}_p$ operator is to choose a grid $\{r_j\}_{j=0}^N$ on the interval $0 \leq r \leq 1$ where

$$0 \leftarrow r_0 < r_1 < r_2 < \ldots < r_j < \ldots < r_N = 1. \tag{4}$$

In the subsequent subsections the derivation of the Buckmire MFD scheme for the cylindrical and spherical cases will be given.

2.1.1 The Cylindrical Case

Consider $B(r)$ which is defined as

$$B(r) = \mathcal{R}_1 u = \frac{rdu}{dr},$$

where $u = u(r)$ is an unknown function (the solution) the operator $\mathcal{R}_1$ acts on. The problem at hand requires determining a numerical discretization or approximation for $\mathcal{R}_1$.

There are several choices for discretizing $B(r)$, the radial derivatives in cylindrical coordinates, on the grid defined in (4). The standard forward-difference (SFD) approximation method and the new nonstandard (MFD) scheme were selected and will be compared with each other. Note that the discrete quantity B is actually defined in between grid points, not on them.

$$B_{j+1/2}^{(SFD)} = r_{j+1/2}\frac{u_{j+1} - u_j}{r_{j+1} - r_j} \tag{5}$$

$$B_{j+1/2}^{(MFD)} = \frac{u_{j+1} - u_j}{\log(r_{j+1}) - \log(r_j)} = \frac{u_{j+1} - u_j}{\log(r_{j+1}/r_j)} \tag{6}$$

The scheme in (5) shall be referred to as the SFD scheme and the new scheme in (6) shall be referred to as the MFD scheme. The MFD scheme can be obtained by assuming that $B(r)$ should be constant on each subinterval (r_j, r_{j+1}) of the grid. If one relates $B(r)$ back to the physical fluid mechanics problem we want to solve, it corresponds to a mass flux. Therefore the condition being imposed is that the mass flux be constant, which is physically appropriate. The relationship between $B_{j+1/2}$ and u_j and u_{j+1} solves the simple boundary value problem

$$ru' = B_{j+1/2} = \text{constant} \tag{7}$$

$$u(r_j) = u_j \tag{8}$$

$$u(r_{j+1}) = u_{j+1}. \tag{9}$$

The solution to this is $u(r) = B_{j+1/2}\log r + C$, which, when one applies the boundary conditions (8) and (9) leads to the formula

$$B_{j+1/2} = \frac{u_{j+1} - u_j}{\log(r_{j+1}/r_j)}.$$

Thus the MFD is a nonstandard, *exact* finite-difference scheme for the ordinary differential equation

$$r\frac{du}{dr} = B, \text{where } B \text{ is a known constant.} \tag{10}$$

2.1.2 The spherical case

In a similar fashion to the procedure outlined above in Section 2.1.1, a nonstandard, exact finite-difference scheme can be obtained for the spherical analogue to (10). The spherical version of the differential equation comes from setting $A(r) = \mathcal{R}_2 u$ equal to a constant, producing

$$r^2 \frac{du}{dr} = A, \text{where } A \text{ is a known constant.} \tag{11}$$

Even though it does not have the same physical significance of a mass flux as it did in cylindrical co-ordinates, we can still obtain a relationship between $A_{j+1/2}$, u_j and u_{j+1} by solving (11) using the conditions (8) and (9). The solution in this case is $u(r) = -A/r + C$, which when one applies the boundary condition leads to the difference equation

$$A_{j+1/2} = \frac{u_{j+1} - u_j}{\left(-\dfrac{1}{r_{j+1}}\right) - \left(-\dfrac{1}{r_j}\right)}.$$

This can be re-arranged to produce

$$A_{j+1/2}^{(MFD)} = r_j r_{j+1} \frac{u_{j+1} - u_j}{r_{j+1} - r_j}. \tag{12}$$

This formula is again an *exact*, nonstandard finite-difference scheme for (11). The SFD scheme for this differential equation would be

$$A_{j+1/2}^{(SFD)} = r_{j+1/2}^2 \frac{u_{j+1} - u_j}{r_{j+1} - r_j}. \tag{13}$$

Notice that in the spherical MFD scheme (12) it is the non-local discretization of r^2 which makes it nonstandard or "Mickens finite difference." In the cylindrical MFD scheme (6) it is the presence of nonlinear functions (logarithms) and the non-local discretization which make it nonstandard. Regardless, both schemes have zero local truncation error; they are exact.

2.2 Informal derivation of the nonstandard schemes

One can also derive the form of the nonstandard schemes given in the previous section by using a more intuitive but less rigorous approach involving

differentials. The differential equation to be approximated is re-arranged through the use of differentials and then the differentials are approximated by finite Δs.

$$B = r\frac{du}{dr} = \frac{du}{\frac{dr}{r}} = \frac{du}{d(\log(r)} \approx \frac{\Delta u}{\Delta(\log(r))}$$

This approximate version of the rearranged ODE is actually the cylindrical MFD (6).

$$\frac{\Delta u}{\Delta(\log(r))} = \frac{u_{j+1} - u_j}{\log(r_{j+1}) - \log(r_j)} = B^{(2)}_{j+1/2}$$

Similarly, one can derive the spherical MFD found in (12) by rearranging the ODE in (11)

$$A = r^2\frac{du}{dr} = \frac{du}{\frac{dr}{r^2}} = \frac{du}{d\left(-\frac{1}{r}\right)} \approx \frac{\Delta u}{\Delta\left(-\frac{1}{r}\right)} = \frac{u_{j+1} - u_j}{\left(-\frac{1}{r_{j+1}}\right) - \left(-\frac{1}{r_j}\right)} = r_j r_{j+1}\frac{u_{j+1} - u_j}{r_{j+1} - r_j} = A^{(2)}_{j+1/2}$$

Conclusion

In this section two very different derivations of MFD schemes which discretize the $\mathcal{R}_p$ operator in cylindrical ($p = 1$) or spherical ($p = 2$) coordinates were given. The new schemes were presented adjacent to the SFD methods for the same Laplacian operator to highlight the unusual features of the nonstandard schemes. In the subsequent sections, both types of schemes will be applied to particular singular boundary value problems and the numerical results will demonstrate the superior utility and versatility of the MFD schemes.

3 MFD Application To Two Singular Linear Boundary Value Problems

Introduction

To illustrate the efficacy and accuracy of the MFD schemes derived in (6) and (12) in Section 2, they are applied to a number of *linear* singular boundary value problems related to the original problem discussed in Buckmire's thesis [6]. These other problems possess the same essential singular nature near the origin due to the nature of the Laplacian operator in cylindrical and spherical coordinates. The reason for the choice of these particular linear singular boundary value problems is that they have easily found exact solutions which involve logarithms or Bessel functions. Thus these problems are highly suitable for the benchmarking of the Buckmire MFD scheme introduced in [6] and discussed in [7], [8] and Section 2. The goal of this section of this paper is to present a brief summary of the results reported in [9] which indicate the utility of MFD schemes for the numerical solution of singular boundary value problems.

3.1 The First Model Problem

The Kármán-Guderley equation (1) and the associated boundary conditions of (2) and (3) can be directly related to the simple boundary value problem given below

$$\frac{1}{r}\frac{d}{dr}\left(r\frac{du}{dr}\right) - m^2 u = 0, \qquad m \text{ constant} \tag{14}$$

$$r\frac{du}{dr}\bigg|_{r=0} = S, \tag{15}$$

$$u(1) = G. \tag{16}$$

This singular boundary value problem has a known exact solution that depends on the value of m, where m is a natural number. The exact solutions to the model boundary value problem in cylindrical coordinates can be written as

$$m = 0, \qquad u(r) = S\log r + G \tag{17}$$

$$m > 0, \qquad u(r) = -SK_0(rm) + (G + SK_0(m))\frac{I_0(rm)}{I_0(m)}. \tag{18}$$

Note that these solutions to the cylindrical model problem have the required singular behavior ($\mathcal{O}(\log r)$) as $r \to 0$.

3.1.1 The $m \neq 0$ cylindrical discretization

When $m \neq 0$ the model differential equation in (14) becomes

$$r^2 u''(r) + r u'(r) - m^2 r^2 u(r) = 0, \tag{19}$$

which after the scaling $s = mr$ can be seen to be the zeroth-order Bessel's equation

$$s^2 u''(s) + s u'(s) - s^2 u(s) = 0.$$

Using a standard discretization, the difference equation for the $m \neq 0$ form of (14) is

$$\frac{1}{r_j}\left(r_{j+1/2}\frac{u_{j+1} - u_j}{r_{j+1} - r_j} - r_{j-1/2}\frac{u_j - u_{j-1}}{r_j - r_{j-1}} \right) - m^2 u_j = 0. \tag{20}$$

Using the Buckmire MFD, the nonstandard discretization will produce

$$\frac{1}{r_j}\left(\frac{u_{j+1} - u_j}{\log(r_{j+1}/r_j)} - \frac{u_j - u_{j-1}}{\log(r_j/r_{j-1})} \right) - m^2 u_j = 0. \tag{21}$$

In the $m \neq 0$ cases, solutions are obtained by solving a tri-diagonal system of equations for $\{u_j\}_{j=0}^{N}$. In the $m \neq 0$ case the nonstandard scheme is not exact, but it can be clearly seen from the numerical results given later that the MFD scheme does a better job of approximating the exact solution than the standard scheme does, especially near the $r = 0$ singularity. Recall, that in the original problem, it is near $r = 0$ that accuracy is most required. Before examining the numerical results of solving the difference equations in (20) and (21), the application of Buckmire's MFD to another model singular boundary value problem will be presented in the next subsection.

3.2 The Second Model Problem

The second model problem (in spherical coordinates) is not directly motivated from the Kármán-Guderley boundary value problem as the cylindrical

version is. It is simply an analogous extrapolation to spherical coordinates from the cylindrical model problem given in (14),

$$\frac{1}{r^2}\frac{d}{dr}\left(r^2\frac{du}{dr}\right) - n^2 u = 0, \qquad n \text{ constant} \tag{22}$$

$$r^2\frac{du}{dr}\bigg|_{r=0} = S, \tag{23}$$

$$u(1) = G. \tag{24}$$

The exact solution of the model spherical differential equation can be found to consist of hyperbolic sines and hyperbolic cosines after noticing that (22) can be rewritten (when $n \neq 0$) as

$$r^2u''(r) + 2ru'(r) - n^2r^2u(r) = 0. \tag{25}$$

This looks very similar to the Bessel's equation from the cylindrical coordinates problem (19), but the solutions are very different. The derivatives can be grouped so that if $v = ru$ the equation becomes

$$\begin{aligned} r^2u'' + 2ru' - n^2r^2u &= (ru)'' - n^2(ru) \\ &= v''(r) - n^2v(r) \\ &= 0 \end{aligned}$$

The general solution to (25) is $u(r) = C_1\dfrac{\sinh(nr)}{r} + C_2\dfrac{\cosh(nr)}{r}$. The exact solutions to the model boundary value problem in spherical coordinates given in (22), (23) and (24) depend on the value of the natural number n and can be written as

$$n = 0, \qquad u(r) = -\frac{S}{r} + S + G \tag{26}$$

$$n > 0, \qquad u(r) = \frac{-S\cosh(nr)\sinh(n) + (G + S\cosh(n))\sinh(nr)}{r\sinh(n)} \tag{27}$$

These solutions above also exhibit singular behavior as $r \to 0$, albeit much more strongly than their cylindrical coordinate counterparts. The solutions in spherical coordinates have singular behavior ($\mathcal{O}(\frac{1}{r})$) as $r \to 0$.

3.2.1 The $n \neq 0$ spherical discretization

Using a standard discretization for the $n \neq 0$ form of (22) is

$$\frac{1}{r_j^2}\left(r_{j+1/2}^2 \frac{u_{j+1}-u_j}{r_{j+1}-r_j} - r_{j-1/2}^2 \frac{u_j - u_{j-1}}{r_j - r_{j-1}}\right) - n^2 u_j = 0. \tag{28}$$

The Buckmire MFD produces a nonstandard discretization which is

$$\frac{1}{r_j^2}\left(r_j r_{j+1} \frac{u_{j+1}-u_j}{r_{j+1}-r_j} - r_j r_{j-1} \frac{u_j - u_{j-1}}{r_j - r_{j-1}}\right) - n^2 u_j = 0. \tag{29}$$

Like the $m \neq 0$ cylindrical case, the solutions to the $n \neq 0$ spherical case are obtained by solving a tri-diagonal system of equations for $\{u_j\}_{j=0}^N$. Fortunately, exact solutions can be found for all values of m (cylindrical cases) and n (spherical cases). In the $n \neq 0$ cases the MFD scheme (29) is not exact, but again the numerical results given later will demonstrate that it does a much better job of approximating the exact solution than the standard scheme (29) does, particularly near the origin.

3.3 Numerical Results

In this subsection the numerical results will be given which indicate the effectiveness of the MFD schemes in approximating the solution to the singular boundary value problems in cylindrical and spherical coordinates. This is done by comparing the solutions to the cylindrical and spherical model problems generated by the numerical schemes given in (20) & (21) and (28) & (29) to the exact solutions given in (18) and (27).

Numerically one can not actually evaluate the Neumann boundary conditions (15) and (23) at $r = 0$ exactly. Instead one chooses a small parameter ϵ and evaluates the boundary condition at $r = \epsilon$ repeatedly with values of ϵ that approach zero. For the results displayed in Figure 1, ϵ=.1, .01, .001, .0001 and .00000001. Figure 1 depicts the error between the exact solution and the numerical solution that each numerical method makes as the Neumann boundary conditions (15) and (23) are approximated at ever smaller values of r ($\epsilon \to 0$) for both the cylindrical and spherical model boundary value problems. The filled dots in the figure represent the error due to the SFD scheme while the empty dots represent the error due to the MFD scheme. Note that in both the cylindrical and spherical case the error due

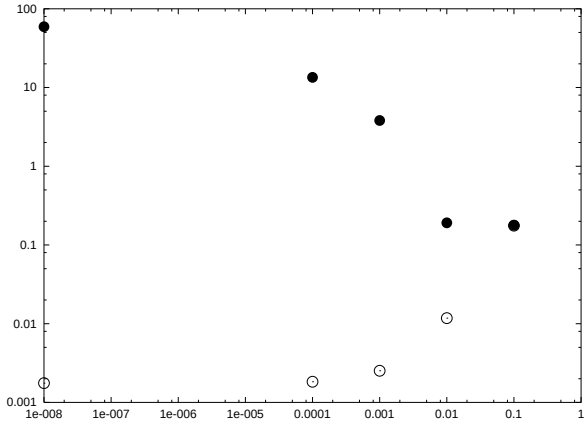

(a) $|u_0 - u_{exact}(0)|$ for $m = 1$

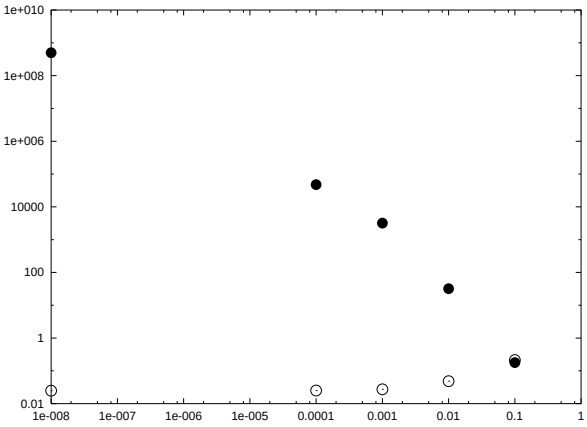

(b) $|u_0 - u_{exact}(0)|$ for $n = 1$

Figure 1: Numerical error at $r = \epsilon \to 0$ for cylindrical ($m = 1$) and spherical ($n = 1$) data

to the MFD scheme near the boundary (i.e. as $\epsilon \to 0$) is consistently smaller than the error due to the SFD scheme. In fact not only are the empty dots beneath the filled dots in both examples, but as ϵ gets smaller the error due to the MFD scheme appears to *decrease* slightly while the error due to the SFD scheme is *increasing*. It is these results which demonstrate the superior ability of the nonstandard scheme to handle the singular nature of the pertinent boundary value problems.

Since the MFD schemes in cylindrical coordinates and spherical coordinates are exact (have zero error) in the $m = 0$ and $n = 0$ cases, respectively they have not been included here but are available in [9]. The two types of finite-difference schemes (standard and nonstandard) approximate the solutions to these problems with wildly varying accuracy, with the MFD scheme being more successful by *orders of magnitude*. At $r = \epsilon = .0001$ the standard scheme produces an error of about 10^2 while the nonstandard scheme produces an error of about 10^{-1}. In Figure 2 the graphs show the error on a log-log scale with each curve representing a solution computed at a different value of ϵ. Notice in Figure 2(b) that the nonstandard scheme's error actually *decreases* as the boundary condition is evaluated at a more singular value closer to the origin, while the reverse is true for the standard scheme in Figure 2(a).

The corresponding graphs of the error made by the two competing schemes in solving the spherical model problem are given below in Figure 3. In Figure 3(a) one can notice that the order of magnitude of the error made by the standard scheme is gigantic ($\approx 10^4$) while in Figure 3(b) it is clear that the nonstandard scheme has only a modest error ($\approx 10^{-1}$), even when the inner boundary condition is being evaluated at the relatively small value of $\epsilon = .0001$.

All the calculations performed in this section used a uniform discrete grid with $N = 101$ grid points, with a grid separation which varied depending on ϵ. The known constants in the boundary conditions were taken to be $G = 2$ and $S = 5$ for no particular reason.

Conclusions

In this section of the paper, MFD schemes have been applied to solve singular boundary value problems with differential equations in cylindrical or spherical coordinates. These model boundary value problems were simplified versions of the original boundary value problem the Buckmire MFD

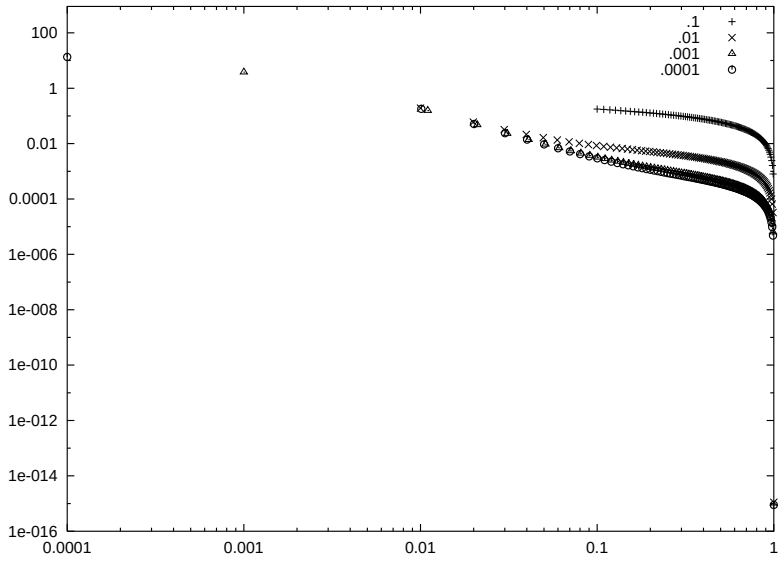

(a) $m = 1$ error using standard finite differences

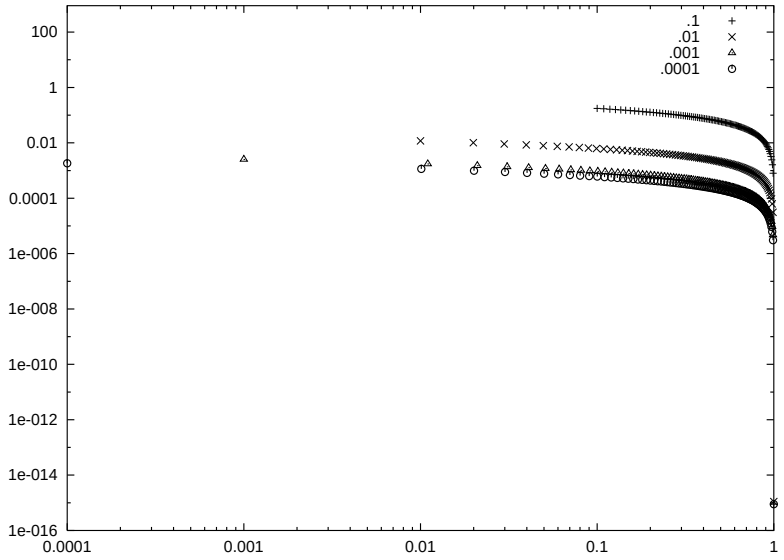

(b) $m = 1$ error using nonstandard finite differences

Figure 2: Numerical error comparison as $\epsilon \to 0$ for cylindrical solutions of (14)

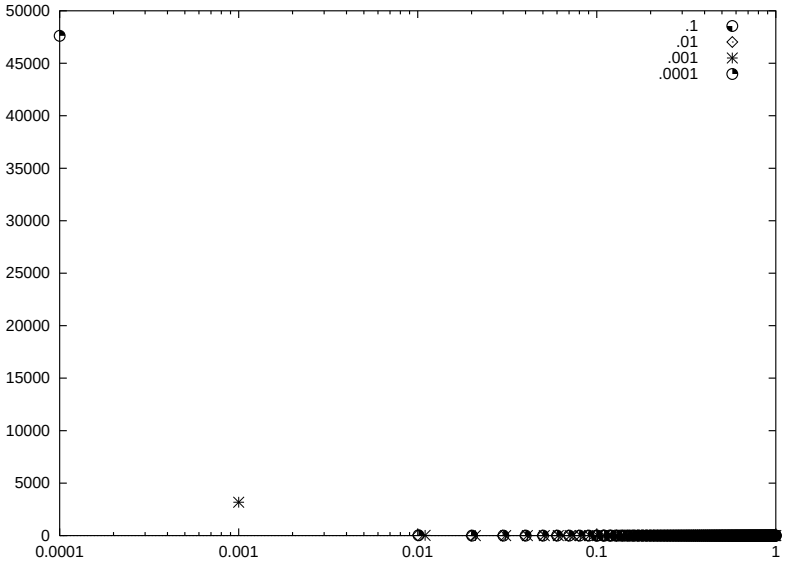

(a) $n = 1$ error using standard finite difference

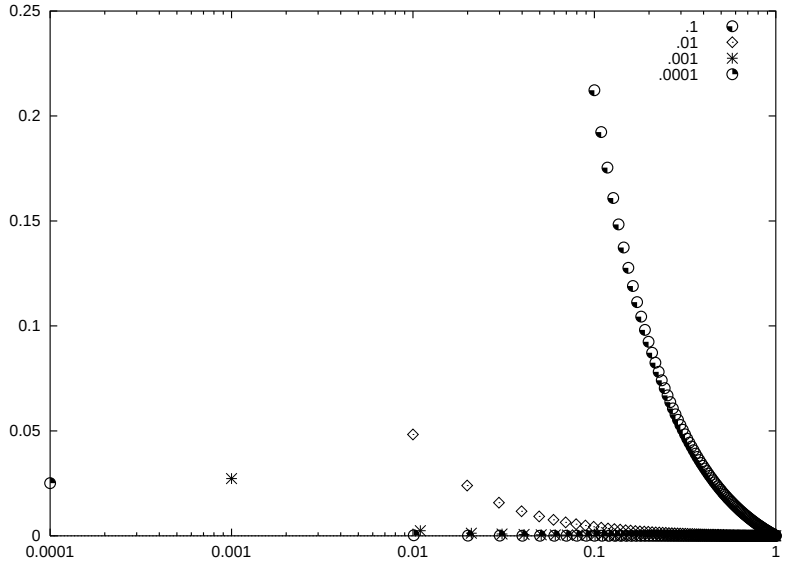

(b) $n = 1$ error using MFD

Figure 3: Numerical error comparison as $\epsilon \to 0$ for spherical solutions of (22)

scheme was first invented for in [6]. The numerical results presented here show that the MFD schemes appear to tackle singular boundary value problems more accurately and efficiently than standard finite-difference schemes. In particular, the nonstandard schemes easily approximate the solution near the singularity at the origin where the standard schemes generally fail and where accuracy of the solution was most desired. In the next section, MFD schemes will be applied to some more singular boundary value problems, related to the ones considered in this section. However, the singular boundary value problem in the next section are nonlinear and possess bifurcations with multiple-valued solutions.

4 MFD Application To The Cylindrical Bratu-Gel'Fand Problem

Introduction

Following application of MFD to a couple of singular linear boundary value problems in the previous section, in this section MFD are applied to a singular nonlinear boundary value problem. The goal of this section of this paper is to present a brief summary of results first reported in [10]. The nonlinear eigenvalue problem $\Delta u + \lambda e^u = 0$ in the unit square with $u = 0$ on the boundary is often referred to as "the classical Bratu problem" or "Bratu's problem." By changing the geometry to a unit circle the classical Bratu problem is known as the Bratu-Gelfand problem [20]. It is a nonlinear eigenvalue problem with two known bifurcated solutions for $\lambda < \lambda_c$, no solutions for $\lambda > \lambda_c$ and a unique solution when $\lambda = \lambda_c$. Due to the nature of the Laplacian operator in cylindrical coordinates, the Bratu-Gelfand problem is also a singular nonlinear boundary value problem and is thus related to the singular linear boundary value problem considered in Section 2.

The Bratu-Gelfand problem can be written as

$$\begin{aligned} u''(r) + \frac{1}{r}u'(r) + \lambda e^{u(r)} = 0 \qquad & 0 \le r \le R, \\ \text{with } u(0) < \infty \quad \text{and} \quad & u(R) = 0. \end{aligned}$$

The exact solution to (30) is given in [36] and is

$$u(r;\lambda) = \ln\left[\frac{b}{\left(1 + \frac{\lambda b}{8}r^2\right)^2}\right], \tag{30}$$

where b is given by

$$b = \frac{32}{\lambda^2 R^4}\left(1 - \frac{\lambda R^2}{4} \pm \sqrt{1 - \frac{\lambda R^2}{2}}\right). \tag{31}$$

Clearly there are only solutions when $\lambda \le \dfrac{2}{R^2}$. When $R = 1$ and more specifity about the inner boundary condition is given (i.e. $u'(0) = 0$) equations

(30) and (31) can be combined to write down the solution to (30) as

$$u(r;\lambda) = \ln\left[\frac{\frac{32}{\lambda^2}\left\{1-\frac{\lambda}{4}\pm\sqrt{1-\frac{\lambda}{2}}\right\}}{\left(1+\frac{4r^2}{\lambda}\left\{1-\frac{\lambda}{4}\pm\sqrt{1-\frac{\lambda}{2}}\right\}\right)^2}\right]. \tag{32}$$

The above expression in (32) has two values for every value of $0 < \lambda < 2$. For example, Figure 4 depicts the bifurcated behavior of the solution by depicting the two solutions for $\lambda = 1$ in relation to the unique solution obtained when $\lambda = 2$. When $\lambda = 1$ the solution obtained from taking the positive square root in (32) when $\lambda = 1$ shall be denoted as $u_+(r;1)$ and $u_-(r;1)$ as the solution obtained when taking the negative square root in (32).

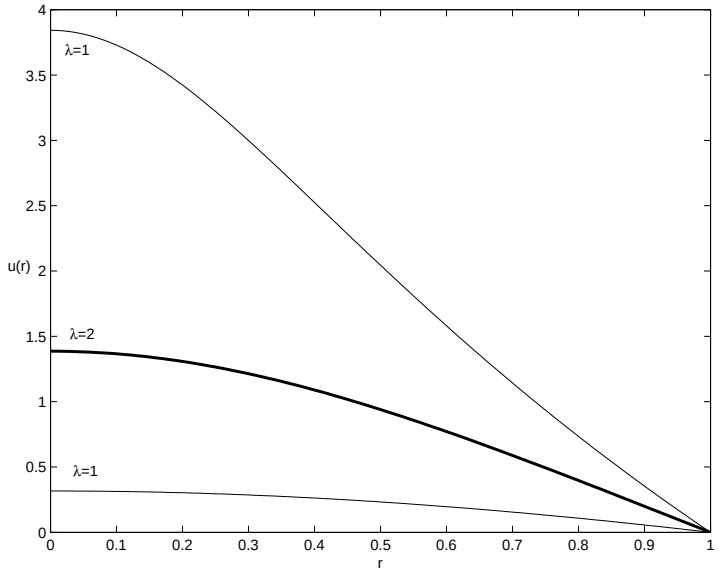

Figure 4: Exact solutions to the Bratu-Gelfand problem when $\lambda = 1$ (bifurcated) and $\lambda = 2$ (unique)

The exact form of the upper curve in Figure 4 is given by

$$u_+(r;1) = \ln\left[\frac{24+16\sqrt{2}}{\left(1+r^2(3+2\sqrt{2})\right)^2}\right] \tag{33}$$

and the exact form of the lower curve is given by

$$u_-(r;1) = \ln\left[\frac{24 - 16\sqrt{2}}{\left(1 + r^2(3 - 2\sqrt{2}\right)^2}\right]. \tag{34}$$

The maximum value $||u||_\infty$ of both curves occurs at $r = 0$, and $u_+(0;1) = \ln(4) + \ln(6 + 4\sqrt{2}) = 3.84218871$ and $u_-(0;1) = \ln(4) + \ln(6 - 4\sqrt{2}) = 0.31669436$.

Another way to illustrate the bifurcated nature of the solution is to graph the maximum value of $u(r)$ on $0 \leq r \leq 1$ versus λ, as shown in Figure 5. This also clearly shows the "turning point" in the solution at the critical value of $\lambda_c = 2$.

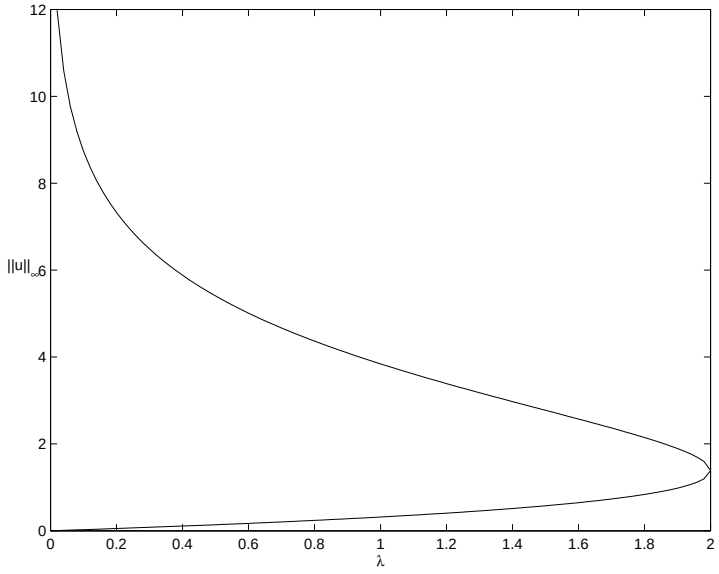

Figure 5: Maximum value of $u(r)$ versus λ depicting the turning point at $\lambda = 2$

The single-valued version of (32) that occurs when $\lambda = 2$ is astonishingly simple:

$$u(r) = \ln\left[\frac{4}{(1 + r^2)^2}\right] = \ln(4) - 2\ln(1 + r^2). \tag{35}$$

The graph of this function (35) is depicted in Figure 6. It is the exact solution to (30) and clearly obeys the boundary conditions $u(1) = 0$ and

$u'(0) = 0$. Note also that its maximum value occurs at $r = 0$ and is exactly $\ln(4) = 1.38629436....$

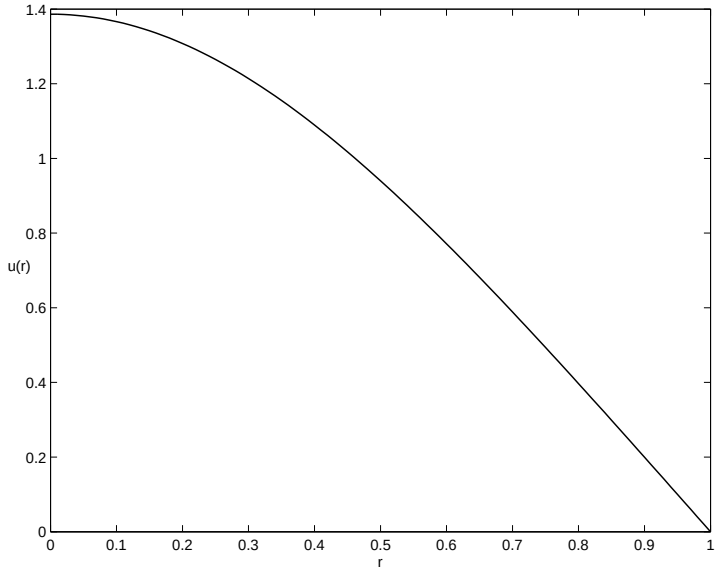

Figure 6: Exact solution of the Bratu-Gelfand problem when $\lambda = 2$

4.1 Numerical Solutions of the Bratu-Gelfand Problem

Standard finite differences and Buckmire's MFD were used to compute numerical solutions to the Bratu-Gelfand problem (30) in order to compare them. Both methods involve forming discrete versions of the boundary value problem by approximating the derivatives and boundary conditions and solving the resulting system of nonlinear difference equations using Newton's Method. The first step in the numerical solution is to discretize the domain of the problem. The grid chosen was $\{r_j\}_{j=0}^{N}$ on the interval $0 \leq r \leq 1$ where

$$0 = r_0 < r_1 < r_2 < \ldots < r_j < \ldots < r_N = 1. \tag{36}$$

For a uniform grid, the grid separation parameter h is constant and $h = 1/N$ with $r_k = 0 + kh$ for $k = 0$ to N. Using the standard finite-difference scheme the discrete version of the Bratu-Gelfand problem (30) will be

$$\frac{1}{r_j}\left(r_{j+1/2}\frac{u_{j+1} - u_j}{r_{j+1} - r_j} - r_{j-1/2}\frac{u_j - u_{j-1}}{r_j - r_{j-1}}\right) + \lambda e^{u_j} = 0. \tag{37}$$

The nonstandard finite-difference scheme for (30) will be

$$\frac{1}{r_j}\left(\frac{u_{j+1}-u_j}{\log(r_{j+1}/r_j)}-\frac{u_j-u_{j-1}}{\log(r_j/r_{j-1})}\right)+\lambda e^{u_j}=0. \tag{38}$$

Note: since this is a singular problem at $r = 0$, r_0 must be positive, i.e. $0 < r_0 << 1$. A simple discrete version of the inner boundary condition $u'(0) = 0$ is

$$\frac{u_1-u_0}{r_1-r_0}=0 \Rightarrow u_1=u_0. \tag{39}$$

Another, more accurate, version of the inner boundary condition is that the flux (i.e. ru') must be zero at the "first" grid point, which when substituted into (37) leads to the following equation at $j = 0$ using standard differencing

$$\frac{1}{r_0}\left(r_{1/2}\frac{u_1-u_0}{r_1-r_0}\right)+\lambda e^{u_0}=0. \tag{40}$$

Using the nonstandard difference method (38) the discrete version of the inner boundary condition is

$$\frac{1}{r_0}\left(\frac{u_1-u_0}{\log(r_1/r_0)}\right)+\lambda e^{u_0}=0. \tag{41}$$

The discrete version of the outer boundary condition $u(1) = 0$ is

$$u_N=0. \tag{42}$$

When $0 < \lambda < 2$ the system of nonlinear equations due to the standard discretization ((37),(40),(42)) and the system due to the Mickens discretization ((38),(41),(42)) are each solved very easily using Newton's Method. Computations are conducted using the exact solution $u(r; 2)$ (35) as an initial guess, with a tolerance of 10^{-8}.

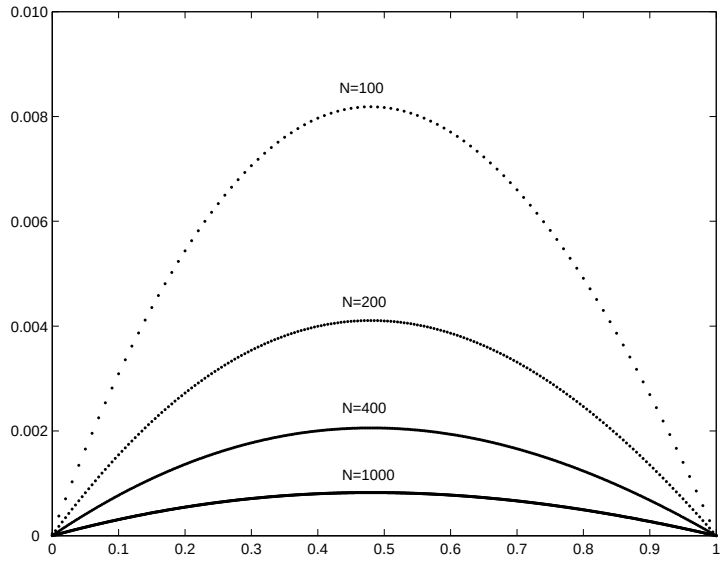

Figure 7: Numerical error versus r for standard method when $\lambda = 1$

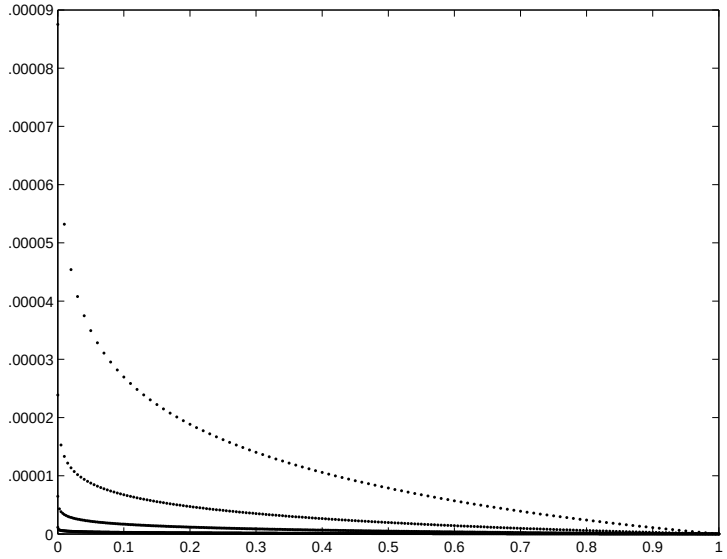

Figure 8: Numerical error versus r for Mickens method when $\lambda = 1$

The numerical errors generated by the two competing methods for $\lambda = 1$ and for various values of increasing N are given in Figure 7 and Figure 8.

Notice the completely different quantitative and qualitative nature of the graphs. The graph in Figure 8 illuminates the error behavior of the non-standard method by using a semilog scale. The smallest maximum error in Figure 7 (the N=1000 curve) is greater than the largest maximum error in Figure 8 (the N=100 curve). Clearly the solution produced by the Mickens scheme has superior accuracy over the one generated using standard finite differences when $\lambda = 1$.

At the turning point $\lambda = 2$ the system of equations generated by using the standard finite difference scheme refuses to converge. This is not unexpected since it is widely known that numerically computing solutions at or near the turning point is difficult using standard methods [26]. However, the Mickens finite-difference method has no problem generating numerical solution at this critical value of the parameter λ.

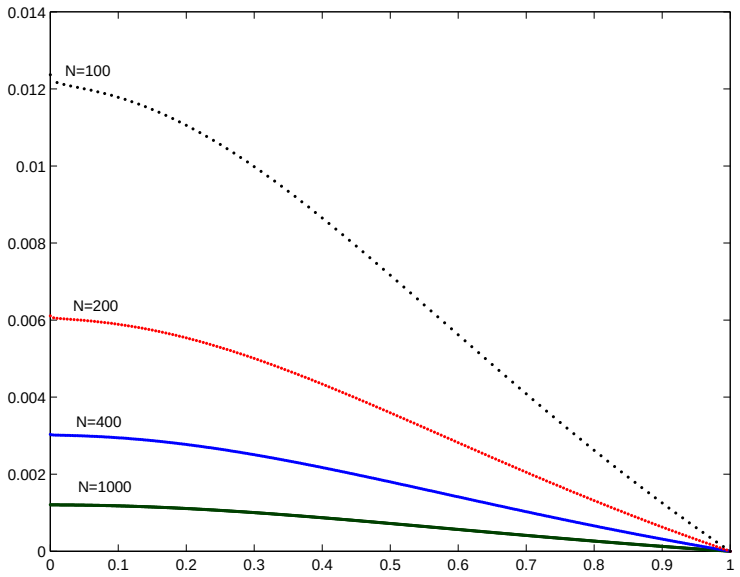

Figure 9: Numerical error using Mickens finite differences with $N = 100, 200, 400$ and 1000 for $\lambda = 2$

The numerical results of solving the Bratu-Gelfand problem at the critical value of $\lambda = 2$ are depicted in Figure 9. This shows that the error is greatest at $r = 0$ (as expected) but that the error over the entire domain $0 \leq r \leq 1$ clearly goes to zero as the number of grid points N increases. These results show the efficacy and versatility of using MFD methods to solve this

singular nonlinear boundary value problem which also happens to possess a double-valued solution. In the next section, the application of MFD to a boundary value problem which is related to the Bratu-Gel'fand problem but is a *non-singular* nonlinear boundary value problem which also happens to have a double-valued solution for values less than a given parameter will be examined.

5 MFD Application To The One-Dimensional Bratu Problem

Introduction

In this section of the paper the results of applying a MFD scheme to a non-singular, nonlinear boundary value problem related to the singular nonlinar problem (also known as the Bratu-Gelfand problem) discussed in Section 4 shall be presented. In this section, a Mickens finite difference is applied to the 1-dimensional planar Bratu problem. This version of the Bratu problem, $u'' + \lambda e^u = 0$ with $u(0) = u(1) = 0$, has two known, bifurcated, exact solutions for values of $\lambda < \lambda_c$ and no solutions for $\lambda > \lambda_c$. The value of λ_c is simply $8(\alpha^2 - 1)$ where α is the fixed point of the hyperbolic cotangent function. The Bratu problem is an elliptic partial differential equation which comes from a simplification of the solid fuel ignition model in thermal combustion theory [19]. It is also a nonlinear eigenvalue problem that is often used as a benchmarking tool for numerical methods ([3], [4], [17]). In [22], Jacobsen and Schmitt provide an excellent summary of the significance and history of the Bratu problem. The goal of this section will be to compare the numerical solutions to the planar one-dimensional Bratu problem produced by MFD to solutions produced by other numerical techniques. The work in this section has not been previously published.

The classical Bratu problem is

$$\Delta u + \lambda e^u = 0 \qquad \text{on } \Omega : \{(x, y) \in 0 \leq x \leq 1, 0 \leq y \leq 1\} \tag{43}$$

$$\text{with } u = 0 \qquad \text{on } \partial\Omega \tag{44}$$

The 1-dimensional (planar) version of this problem is

$$u''(x) + \lambda e^{u(x)} = 0 \qquad 0 \leq x \leq 1, \tag{45}$$

$$\text{with } u(0) = 0 \qquad \text{and } u(1) = 0 \tag{46}$$

In section 5.1 of this paper the exact solution of the one-dimensional planar Bratu problem will be presented. Details of the bifurcated nature of the solution are given. In Section 5.2 brief explanations of the various methods chosen to solve the will be presented. In Section 5.3 numerical solutions generated using Mickens finite differences will be compared to solutions produced using different numerical methods: standard finite differences, a pseudospectral method due to Boyd [4] and the Adomian polynomial decomposition

algorithm [17]. All of the approximate solutions are compared to the exact solution. This section shall conclude with some overall comments and observations based on the numerical result.

5.1 The 1-dimensional Planar Bratu Problem

The exact solution to (45) is given in [3] and [17] and presented here as

$$u(x) = -2\ln\left[\frac{\cosh((x-\frac{1}{2})\frac{\theta}{2})}{\cosh(\frac{\theta}{4})}\right] \tag{47}$$

where θ solves

$$\theta = \sqrt{2\lambda}\cosh\left(\frac{\theta}{4}\right). \tag{48}$$

There are two solutions to (48) for values of $0 < \lambda < \lambda_c$. For $\lambda > \lambda_c$ there are no solutions. Note that this property is similar to the Bratu-Gel'fand problem discussed in Section 4. The solution (47) is only unique for a critical value of $\lambda = \lambda_c$ which solves

$$1 = \sqrt{2\lambda_c}\sinh\left(\frac{\theta_c}{4}\right)\frac{1}{4}. \tag{49}$$

By graphing the line $y = \theta$ and the curve $y = \sqrt{2\lambda}\cosh(\frac{\theta}{4})$ for fixed values of $\lambda = 1, 2, 3, 4$ and 5 the solutions of (48) can be seen as the two points of intersections of the curve and the line in Figure 10. Clearly, there is only one solution when the $y = \theta$ line is exactly tangential to the $y = \sqrt{2\lambda}\cosh(\frac{\theta}{4})$ curve, which leads to the condition given in (49).

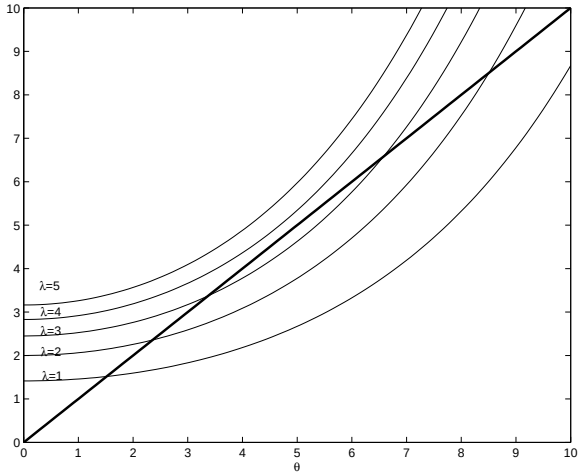

Figure 10: Graphical depiction of dependence of solutions of (48) upon λ

Dividing (49) by (48) produces:

$$\begin{aligned} \frac{4}{\theta_c} &= \tanh\left(\frac{\theta_c}{4}\right) \\ \Rightarrow \frac{\theta_c}{4} &= \coth\left(\frac{\theta_c}{4}\right) \\ \Rightarrow \alpha &= \coth(\alpha) \end{aligned}$$

The critical value θ_c is four times α, which is the positive fixed point of the hyperbolic cotangent function, 1.19967864.

$$\theta_c = 4.79871456 \tag{50}$$

The exact value of θ_c can therefore be used in (49) to obtain the exact value of λ_c.

$$\lambda_c = \frac{8}{\sinh^2\left(\frac{\theta_c}{4}\right)} = 8(\alpha^2 - 1) \Rightarrow \lambda_c = 3.513830719 \tag{51}$$

The relationship between λ and θ for some values of λ less than λ_c are given in Table 5.1. Obviously, when $\lambda = \lambda_c$ then $\theta_1 = \theta_2 = \theta_c$ and when $\lambda > \lambda_c$ there are no solutions to (48).

λ	θ_1	θ_2
0.5	1.0356946	13.0382393
1.0	1.5171645	10.9387028
1.5	1.9397652	9.5816998
2.0	2.3575510	8.5071995
2.5	2.8115549	7.5480981
3.0	3.3735077	6.5765692
3.5	4.5518536	5.0543427
λ_c	4.7987146	4.7987146

Table 1: Corresponding values of θ for various $\lambda \leq \lambda_c$

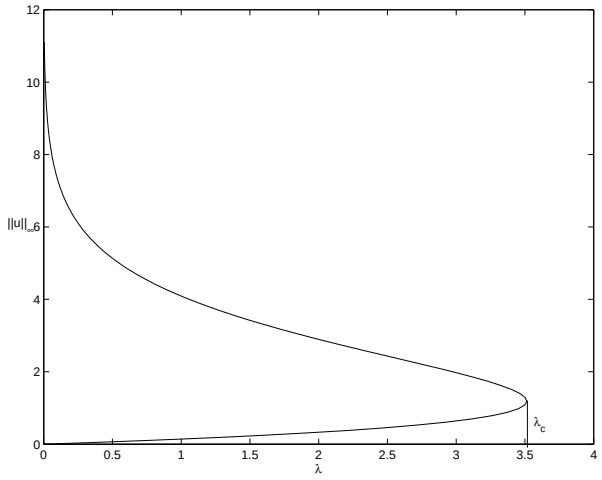

Figure 11: Bifurcated nature of the exact solution to the 1-D Bratu problem

Figure 11 shows how the maximum value of the solution function (47) depends on the nonlinear eigenvalue λ with the critical value of λ_c highlighted at the "turning point." Notice how similar the bifurcation diagram in Figure 11 resembles the bifurcation diagram in Figure 5. Table 5.1 and Figure 11 are two different ways of depicting the property of the solution that it is double-valued for $\lambda < \lambda_c$. In the next subsection, numerical methods to compute these solutions to (45) are presented.

5.2 Numerical Methods

In this section the details of various numerical methods used to compute solutions to (45) shall be given. The first method involves approximating the differential equation with finite differences. Both standard and nonstandard (Mickens) finite-difference schemes are used. In addition to the methods which use finite-differences, two pseduospectral methods are used. The first, due to Boyd [4], uses Gegenbauer polynomials as basis functions. The second, due to Adomian [2] assumes the solution can be represented as an infinite series of polynomials. Lastly the problem was also solved using a shooting method easily available in `Matlab`.

5.2.1 Finite Difference Methods

To solve a boundary value problem using finite differences involves discretizing the differential equation and boundary conditions. This method transforms the problem into a system of simultaneous nonlinear equations which are then usually easily solved using Newton's method. There are many choices for how to approximate the derivatives which appear in a differential equation. The first step in the computation of the numerical solution of (45) using a finite-difference method is to approximate the continuous domain of the problem with a discrete grid. The grid chosen was $\{x_j\}_{j=0}^{N}$ on the interval $0 \leq x \leq 1$ where

$$0 = x_0 < x_1 < x_2 < \ldots < x_j < \ldots < x_N = 1. \tag{52}$$

For a uniform grid, the grid separation parameter h is constant and $h = 1/N$ with $x_k = 0 + kh$ for $k = 0$ to N. Using a standard finite-difference scheme, the discrete version of the planar Bratu problem (45) will be

$$\frac{u_{j+1} - 2u_j + u_{j-1}}{h^2} + \lambda e^{u_j} = 0, \qquad j = 1, 2, \ldots, N-1 \tag{53}$$

A nonstandard finite-difference scheme for (45) is

$$\frac{u_{j+1} - 2u_j + u_{j-1}}{2\ln[\cosh(h)]} + \lambda e^{u_j} = 0, \qquad j = 1, 2, \ldots, N-1 \tag{54}$$

The boundary conditions given in (46) become

$$u_0 = u_N = 0. \tag{55}$$

The discretization given in (54) is another example of a MFD. The nonstandard finite difference scheme given in (54) is a MFD for the second derivative

$$u'' \approx \frac{u_{j+1} - 2u_j + u_{j-1}}{\phi(h)}$$

where the denominator function $\phi(h) = 2\ln[\cosh(h)] = h^2 + o(h^2)$. Thus, in the limit as $h \to 0$ the standard finite-difference scheme (53) and the Mickens finite-difference scheme (54) will be identical. However, for the finite values of h at which numerical computations are conducted the hypothesis is that the nonstandard form of the denominator function $\phi(h)$ will lead to improved accuracy for the Micken finite difference over the standard finite difference.

5.2.2 Boyd collocation

Boyd [4] developed a pseudospectral method to produce approximate solutions to the classical two-dimensional planar Bratu problem

$$\frac{\partial^2 u}{\partial x^2} + \frac{\partial^2 u}{\partial y^2} + \lambda e^u = 0 \text{ on } \{(x, y) \in -1 \leq x \leq 1, -1 \leq y \leq 1\} \tag{56}$$

with $u = 0$ on the boundary of the square. The basic idea is that the unknown solution $u(x, y)$ can be completely represented as an infinite series of spectral basis functions

$$u(x, y) = \sum_{k=1}^{N} a_k \phi_k(x, y). \tag{57}$$

The basis functions $\phi_k(x, y)$ are chosen so that they obey the boundary conditions and have the property that the more terms of the series that are kept, the more accurate the representation of the solution $u(x, y)$ is. In other words, as $N \to \infty$ the error diminishes to zero. For finite N the series expansion in (57) is substituted into (56) to produce the residual R. The residual function will depend on the spatial variables (x, y), the unknown coefficients a_k and the parameter λ. The goal of Boyd's pseudospectral method is to find a_k so that the residual function R is zero at N "collocation points." The collocation points are usually chosen to be the roots of orthogonal polynomials that fall into the same family as the basis functions $\phi_k(x, y)$. Boyd [4] uses the Gegenbauer polynomials to define the collocation points. The Gegenbauer polynomials [18] are orthogonal on the interval $[-1, 1]$ with respect to the weight function $w(x) = (1 - x^2)^b$ where $b = -1/2$ corresponds to the

Chebyshev polynomials and $b = 1$ is the choice Boyd uses. The second-degree Gegenbauer polynomial is

$$G_2(x) = \frac{3}{2}(5x^2 - 1), \qquad -1 \leq x \leq 1. \tag{58}$$

In other words, using a 1-point collocation method at the point $x_1 = \left(\frac{1}{\sqrt{5}}, \frac{1}{\sqrt{5}}\right)$ and the choice of
$\phi_1(x, y) = (1 - x^2)(1 - y^2)$ Boyd is able to obtain an approximation to the value of λ_c with a relative error of 8% [4]. Note that this choice for $\phi_1(x, y)$ satisfies the boundary conditions (44) since $\phi(1, y) = \phi(-1, y) = \phi(x, -1) = \phi(x, 1) = 0$.

In the rest of this section Boyd's collocation method described above for Bratu's problem in planar two-dimensional coordinates (56) shall be extrapolated to solve the planar one-dimensional Bratu probem (45). The most obvious difference is the change in the domain from a square $[-1, 1] \times [-1, 1]$ to an interval $[0, 1]$. Using a linear transformation of $z = \frac{x + 1}{2}$ the Gegenbauer polynomial $G_2(x)$ defined on $[-1, 1]$ found in (58) becomes

$$G_2(2z - 1) = 6(1 - 5z + 5z^2), \qquad 0 \leq z \leq 1. \tag{59}$$

The corresponding collocation point to x_1 becomes $z_1 = \frac{1}{10}(5 + \sqrt{5})$ with $\phi_1(z) = z(1 - z)$ and assuming $u(z) = A\phi_1(z)$. (Note this form of $\phi(z)$ satisfies the boundary conditions that $\phi(0) = \phi(1) = 0$.) Substituting z_1 and $\phi_1(z)$ into the one-dimensional planar Bratu problem (replace x by z) produces an equation for the residual which is constrained to be zero.

$$R[z_1; \lambda, A] = R[\frac{1}{10}(5 + \sqrt{5}); \lambda, A] = -2A + \lambda e^{\frac{1}{5}A} = 0 \tag{60}$$

Solving (60) for λ produces

$$\lambda_1(A) = 2Ae^{-0.2A} \tag{61}$$

The expression (61) attains its maximum value of λ_c at $A = 5$. In other words, using 1-point Boyd collocation produces an estimate of $\lambda_c = 10e^{-1} = 3.67879441$ which is 4.7% greater than the exact value of $\lambda_c = 3.513830719$.

To increase accuracy the number of collocation points is increased. However, the number of residual equations (and their complexity) will simultaneously also increase. Using 2-point collocation the form of $u(x)$ is assumed to be

$$u(z) = A\phi_1(z) + B\phi_2(z) = Az(1-z) + Bz(1-z)(2z-1)^2, \qquad 0 \le z \le 1. \tag{62}$$

The above two-point collocation expansion corresponds to the expansion $u(x) = A(1-x^2) + Bx^2(1-x^2)$ which would be valid on $[-1,1]$. The fourth-degree Gegenbauer polynomial, defined on $[-1,1]$ is

$$G_4(x) = \frac{15}{8}(1 - 14x^2 + 21x^4), \qquad -1 \le x \le 1 \tag{63}$$

which on transformation to $[0,1]$ becomes

$$G_4(2z-1) = 15(1 - 14z + 56z^2 - 84z^3 + 42z^4), \qquad 0 \le z \le 1 \tag{64}$$

$G_4(x)$ has four roots on the interval $[-1,1]$ symmetrically distributed around the origin. The two largest roots are selected as the collocation points for the 2-point Boyd collocation method. The two residual equations are formed by substituting (62) into the planar Bratu equation at the collocation points.

$$\begin{aligned} R\left[\frac{1}{42}\left(21 + \sqrt{21(7-2\sqrt{7})}\right); \lambda, A, B\right] &= -8A - 8B + \frac{32B}{\sqrt{7}} + \lambda e^{\frac{2}{63}(21A + 3\sqrt{7}A + 5B - \sqrt{7}B)} = 0 \\ R\left[\frac{1}{42}\left(21 + \sqrt{21(7+2\sqrt{7})}\right); \lambda, A, B\right] &= -8A - 8B - \frac{32B}{\sqrt{7}} + \lambda e^{\frac{2}{63}(21A - 3\sqrt{7}A + 5B + \sqrt{7}B)} = 0 \end{aligned}$$

The method of solution is to find closed-form expressions for λ and B in terms of either A. This is not easy to do with the system as currently constituted. However by eliminating terms in the exponentials which are significantly smaller than the other terms it turns out that a closed form expression for $\lambda(A)$ obtained from the 2-point Boyd collocation method can be found.

$$\lambda_2(A) = \frac{64\sqrt{7}Ae^{\frac{2}{21}(-7+\sqrt{7})A}}{-7 + 4\sqrt{7} + (7 + 4\sqrt{7})e^{\frac{4A}{3\sqrt{7}}}} \tag{65}$$

The maximum value of the expression (65) is $\lambda_c = 3.45611039$, which is only 1.64% smaller than the exact value (51).

5.2.3 Adomian polynomial decomposition

Adomian [2] developed a "polynomial decomposition" method of representing solutions to boundary value problems of the form

$$\begin{array}{ccc} u'' & = & -F(u) \\ u(0) = \alpha & \text{and} & u(1) = \beta. \end{array}$$

The exact solution to (5.2.3) can be represented by a Green's Function

$$u(x) = \lambda \int_0^1 g(x,s)F(u(s))ds + (1-x)\alpha + \beta x \tag{66}$$

where

$$g(x,s) = \begin{cases} s(1-x), & 0 \le s \le x \\ x(1-s), & x \le s \le 1. \end{cases} \tag{67}$$

Adomian's decomposition method assumes that the unknown solution $u(x)$ and the given nonlinear functional $F(u)$ can each be represented as infinite series.

$$u = \sum_{i=0}^{\infty} u_i = u_0 + u_1 + u_2 + \ldots \tag{68}$$

and

$$F(u) = \sum_{i=0}^{\infty} A_i = A_0 + A_1 + A_2 + \ldots. \tag{69}$$

In the case of $F(u)$ the infinite series is a Taylor Expansion about u_0. In other words

$$F(u) = F(u_0) + F'(u_0)(u-u_0) + F''(u_0)\frac{(u-u_0)^2}{2} + F^{(3)}(u_0)\frac{(u-u_0)^3}{3} + \ldots \tag{70}$$

By re-writing (68) as $u - u_0 = u_1 + u_2 + u_3 + \ldots$, substituting it into (70) and then equating the two expressions for $F(u)$ found in (70) and (69) defines formulas for the "Adomian polynomials."

$$F(u(s)) = A_0 + A_1 + A_2 + \ldots = F(u_0) + F'(u_0)(u_1 + u_2 + u_3 + \ldots) + F''(u_0)\frac{(u_1 + u_2 + u_3 + \ldots)^2}{2!} + \ldots \tag{71}$$

By equating terms in (71) the first few Adomian polynomials A_0, A_1, A_2 are given...

$$\begin{aligned}
A_0 &= F(u_0) \\
A_1 &= u_1 F'(u_0) \\
A_2 &= u_1^2 F''(u_0)/2! + u_2 F'(u_0) \\
A_3 &= u_1^3 F^{(3)}(u_0)/3! + 2u_1 u_2 F''(u_0)/2! + u_3 F'(u_0) \\
A_4 &= u_1^4 F^{(4)}(u_0)/4! + 3u_1^2 u_2 F^{(3)}(u_0)/3! + (2u_1 u_3 + u_2^2) F''(u_0)/2! + u_4 F'(u_0)
\end{aligned}$$

Now that the $\{A_k\}_{k=0}^{\infty}$ are known, (69) can be substituted in (66) to specify the terms in the expansion for the solution (68).

$$\begin{aligned}
u(x) &= \lambda \int_0^1 g(x,s) \sum_{i=0}^{\infty} A_i \, ds + (1-x)\alpha + \beta x \\
\sum_{i=0}^{\infty} u_i &= \alpha(1-x) + \beta x + \lambda \sum_{i=0}^{\infty} \int_0^1 g(x,s) A_i \, ds
\end{aligned}$$

Equating the terms yields

$$\begin{aligned}
u_0 &= \alpha(1-x) + \beta x \\
u_1 &= \lambda \int_0^1 g(x,s) A_0(s) ds \\
u_2 &= \lambda \int_0^1 g(x,s) A_1(s) ds \\
&\vdots \qquad \vdots \\
u_k &= \lambda \int_0^1 g(x,s) A_{k-1}(s) ds
\end{aligned}$$

Now the $\{u_k\}_{k=0}^{\infty}$ are known, so the solution is given by $u = u_0 + u_1 + u_2 + u_3 + \ldots$.

To apply the Adomian polynomial decomposition method to solve the one-dimensional planar Bratu problem (45) involves setting $\alpha = \beta = 0$ and $F(u) = e^u$. A happy accident is that the k^{th} derivative of $F(u)$, $F^{(k)}(u) = e^u$ so that choosing $u_0 = 0$ greatly simplifies the formulas for the Adomian

polynomials $\{A_k\}$ since $e^{u_0} = 1$.

$$\begin{aligned}
A_0 &= 1 \\
A_1 &= u_1 \\
A_2 &= u_1^2/2! + u_2 \\
A_3 &= u_1^3/3! + u_1 u_2 + u_3 \\
A_4 &= u_1^4/4! + u_1^2 u_2/2 + u_1 u_3 + u_2^2/2! + u_4 \\
&\vdots \quad\quad \vdots
\end{aligned}$$

Knowing the $\{A_k\}$ terms leads to the calculation of the $\{u_k\}$ terms

$$\begin{aligned}
u_0 &= 0 \\
u_1 &= \lambda \int_0^1 g(x,s) \cdot 1 \; ds = \lambda \int_0^x s(1-x) \; ds + \lambda \int_x^1 x(1-s) \; ds \\
&= \frac{1}{2}(1-x)x\lambda \\
u_2 &= \lambda \int_0^1 g(x,s) \cdot \frac{1}{2}(1-s)s\lambda \; ds \\
&= \lambda^2(1-x) \int_0^x \frac{1}{2}(1-s)s^2 \; ds + \lambda^2 x \int_x^1 \frac{1}{2}(1-s)^2 s \; ds \\
&= \frac{1}{24}(1 - 2x^2 + x^3)x\lambda^2 \\
u_3 &= \lambda \int_0^1 g(x,s) \cdot A_2(s) \; ds \\
&= \frac{1}{1440}(9 - 10x^2 - 15x^3 + 24x^4 - 8x^5)x\lambda^3 \\
u_4 &= \lambda \int_0^1 g(x,s) \cdot A_3(s) ds \\
&\vdots \quad\quad \vdots
\end{aligned}$$

5.2.4 Shooting Method

The last and probably the most obvious method used to obtain a numerical solution of the planar Bratu problem is the nonlinear shooting method. This

involves converting the nonlinear boundary value problem (45) into a system of nonlinear initial value problems which look like

$$\frac{d}{dt}\vec{y} = \vec{f}(\vec{y}), \qquad \vec{y}(0) = \vec{y}_0,$$

with the choice of $\vec{y} = \begin{bmatrix} y_1 \\ y_2 \\ y_3 \\ y_4 \end{bmatrix}$, $\vec{f} = \begin{bmatrix} f_1(\vec{y}) \\ f_2(\vec{y}) \\ f_3(\vec{y}) \\ f_4(\vec{y}) \end{bmatrix} = \begin{bmatrix} y_2 \\ -e^{y_1} \\ y_4 \\ -e^{y_3} \end{bmatrix}$ and $\vec{y}_0 = \begin{bmatrix} 0 \\ s_0 \\ 0 \\ 1 \end{bmatrix}$.

The shooting method works by choosing a value s_0 for $u'(0)$, solving the initial value problem (using a standard ODE solver like Runge-Kutta) and then comparing the value of $y_1(b)$ with the expected value of $u(b) = 0$. A new value of s_k is chosen by using Newton's Method, where

$$s_{k+1} = s_k - \frac{y_1(b) - u(b)}{y_3(b)} \tag{72}$$

The method is said to converge when the difference between subsequent values of s_k fall below a given tolerance, in other words $y_1(b)$ is very close to $u(b)$.

In the next subsection, the results of using the numerical methods detailed in this section are given.

5.3 Numerical Results

The results of applying various numerical methods to produce solutions of the planar one-dimensional Bratu problem (45) are given in this section. We shall begin with considering the results obtained using finite differences. A comparison of the errors generated using Mickens finite differences and standard finite differences are illustrated in Figure 12. By examining Figure 12 it can be observed that the error due to each finite difference method decreases proportionally to with $h^2 = \frac{1}{N^2}$. Also note that the Mickens finite difference error (solid line) is consistently smaller than the standard discretization error (dashed line). The value of the parameter λ shall be taken to be one.

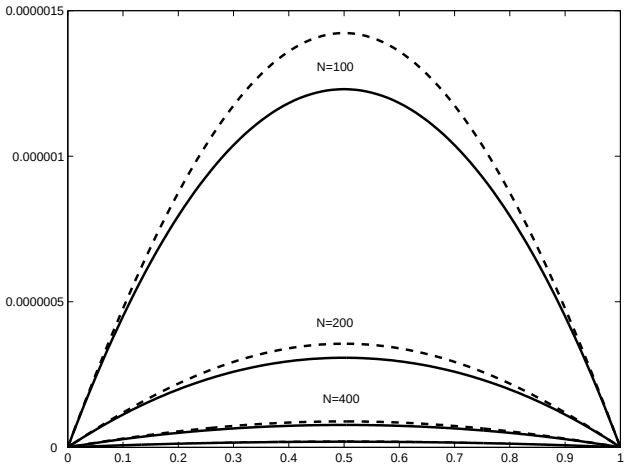

Figure 12: Comparison of standard error and Mickens error for $N = 100, 200, 400$ and 800 when $\lambda = 1$

Interestingly, despite the fact that there are two solutions to (45) at $\lambda = 1$ as shown in Figure 13, the standard finite difference scheme will only converge to one of them, the "lower" solution, i.e. the one below the $\lambda = \lambda_c$ solution. The MFD scheme will converge to either solution, depending on the initial guess chosen for all values $0 < \lambda < \lambda_c$. Neither discretization method will converge to the unique solution at $\lambda = \lambda_c$. Note that this is different behavior than what happened when standard finite differences and MFD were used to solve the Bratu-Gel'fand problem in Section 4. There, the MFD scheme converged at $\lambda = \lambda_c$ but the standard finite difference scheme did not.

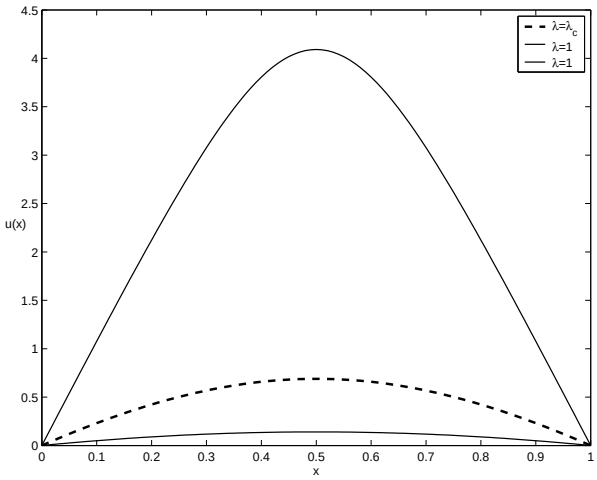

Figure 13: The two solution curves for $\lambda = 1$ and the unique solution curve for $\lambda = \lambda_c$

The solution produced by Boyd's pseudospectral method does not have the deficiency of being unable to converge to both solutions of the Bratu problem for $\lambda < \lambda_c$ which the standard finite-difference method and Adomian decomposition method both have. Boyd's method is able to produce continuous expressions for λ versus the maximum value of the solution. In Figure 14 the behavior of Boyd solutions produced using 1-point and 2-point collocation is compared with the exact solution's bifurcated behavior (as depicted in Figure 11), which indicates the multivalued nature of the Boyd solutions.

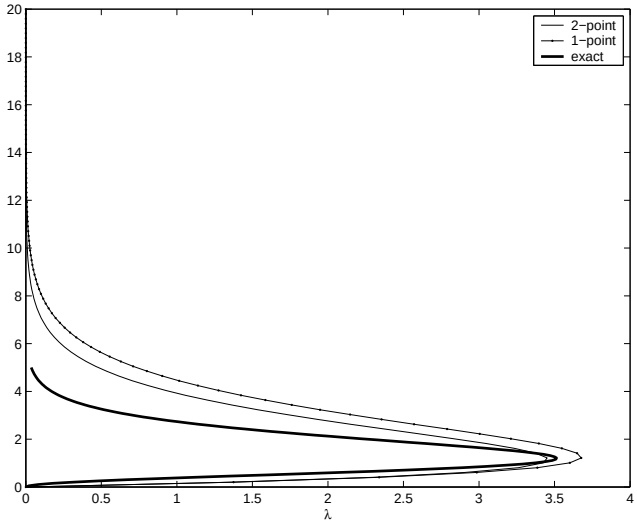

Figure 14: Dependence of Boyd pseudospectral solutions on λ

When $\lambda = 1$ there are two solutions to the Bratu problem (45), which are depicted in Figure 13 and called the "upper" solution and the "lower" solution. In Figure 15 the results of producing solutions using Boyd's pseudospectral method to the Bratu problem when $\lambda = 1$ are depicted. The exact solution is the dark solid line, with the solution from the 1-point collocation depicted using a continuous dotted line and the solution from the 2-point collocation depicted using a continuous solid line. Interestingly, Boyd's method does very well with just 1-point collocation to approximate the lower solution. The 1-point Boyd collocation method doesn't do a very good job of approximating the solution to the "upper" Bratu solution, though the 2-point Boyd collocation does much better, as seen in Figure 15. This is not a surprise, since the expectation is that using more collocation points will decrease the error. By looking at Figure 14 it is clear that at $\lambda = 1$ the three curves (exact solution, 1-point and 2-point) are close together at the lower arc of the bifurcation curve corresponding to the "lower solution" and they are not close together at the upper arc of the bifurcation curve corresponding to the "upper solution." The proximity of the curves is indicative of the numerical error, and the error in approximating the lower solution is smaller than the error in approximating the upper solution.

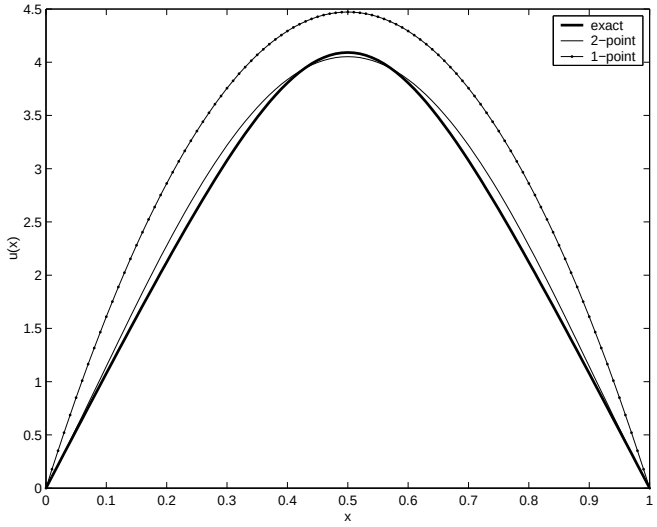

(a) Upper solution when $\lambda = 1$

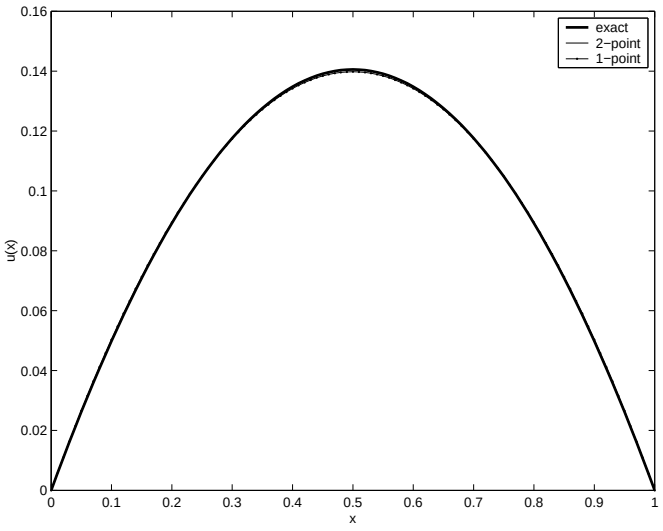

(b) Lower solution when $\lambda = 1$

Figure 15: Comparison of Boyd solutions generated by one-point and two-point collocation

The solutions generated by the Adomian polynomial decomposition only approach the exact solution for small values of $\lambda \leq 1$. Like the standard

discretization method, the Adomian method's solution only converges to the "lower" solution at $\lambda = 1$. In Figure 16 the first three nonzero terms of the Adomian polynomial expansion (solid curves) are depicted next to the exact solution (unconnected dotted line). Clearly, these terms $(u_1 + u_2 + u_3)$ are enough to approximate the exact solution relatively accurately when $\lambda = 1$. However, if $\lambda = \lambda_c$ is selected one needs far more than three terms of the series $\{u_k\}_{k=0}^{\infty}$ to converge to the exact solution, as can be seen in Figure 16. Deeba et. al. [17] obtained identical results when they applied Adomian's polynomial decomposition method to the same boundary value problem (45).

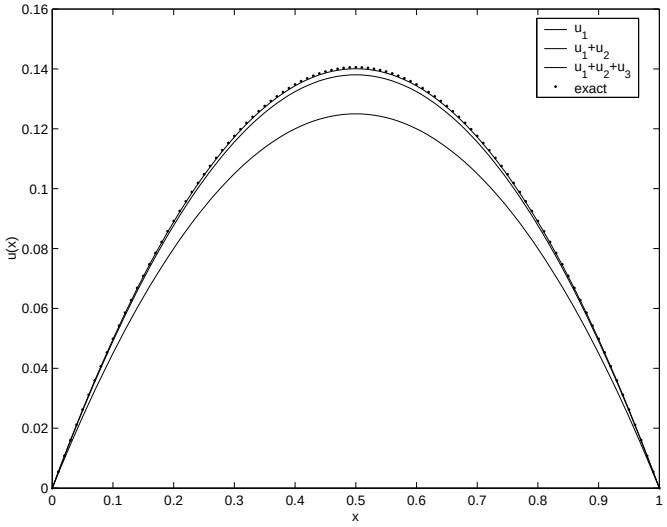

(a) Adomian polynomial solution for $\lambda = 1$

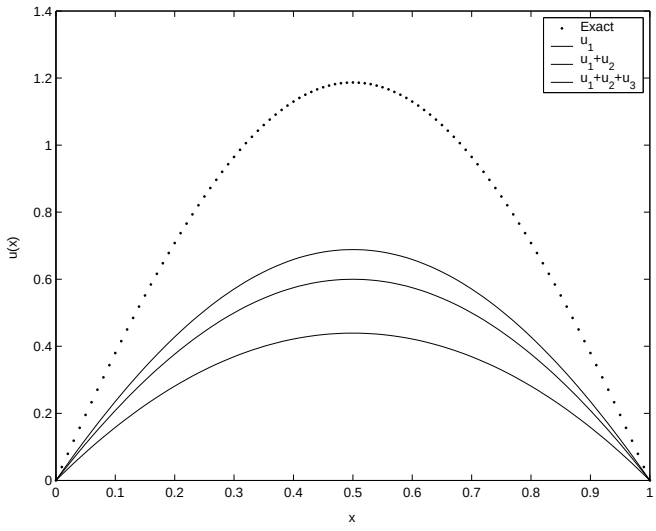

(b) Adomian polynomial solution for $\lambda = \lambda_c$

Figure 16: Comparison of using first three non-zero terms of Adomian polynomial solution for $\lambda = 1$ and $\lambda = \lambda_c$

The shooting method was implemented using the MATLAB routine `ode45` and produces accurate numerical solutions rapidly for values of $\lambda < \lambda_c$. The

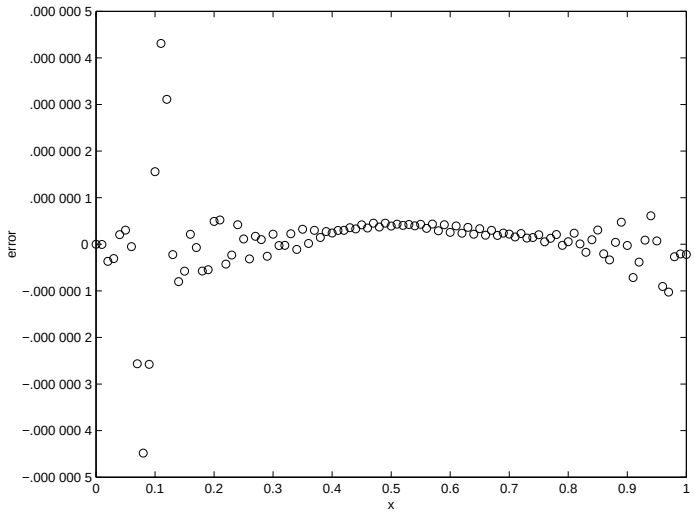

(a) Error due to nonlinear shooting for $\lambda = 1$ "upper" solution

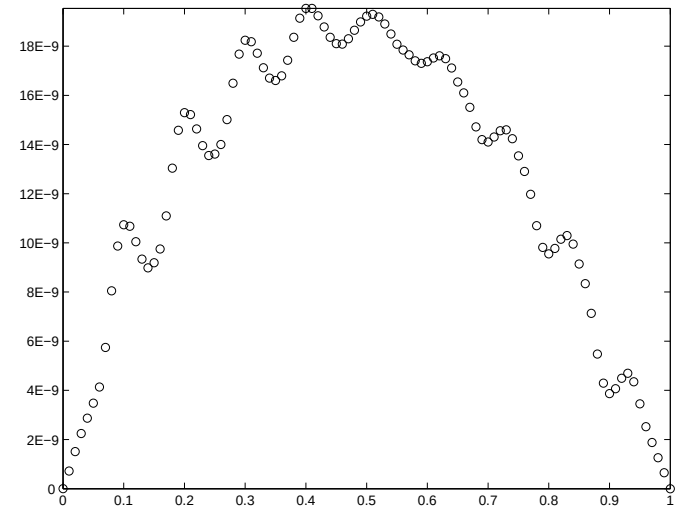

(b) Error due to nonlinear shooting for $\lambda = 1$ "lower" solution

Figure 17: Errors generated by the nonlinear shooting method when $\lambda = 1$ using $N = 100$

shooting method will converge to both the upper and lower solutions depicted in Figure 13 by carefully choosing the value of the initial slope s_0 in (72). However, when $\lambda = \lambda_c$, like the finite-difference methods in Section 5.2.1, the shooting method will not converge to a solution within the given tolerance. Figure 17 depicts the numerical error produced by the nonlinear shooting method as it approximates both Bratu solutions at $\lambda = 1$. Since the numerical error of the shooting method depends on the tolerance of the ODE solver, and not the grid separation, N was chosen to be 100 with a `RelTol` of 10^{-10}.

Conclusion

Five different methods were used to generate numerical solutions of the planar one-dimensional Bratu problem. The five methods were, two finite-difference methods, two spectral methods and a nonlinear shooting method. The methods were chosen for their ease of use for relative error generated. This is why only a few terms (two in the case of the Boyd pseudospectral method and three in the case of the Adomian polynomial decomposition) were used. Only the Mickens discretization and the nonlinear shooting method had no difficulty handling the bifurcated nature of the solution for subcritical values of the parameter λ. The Adomian and Boyd methods do successfully approximate the "lower" of the multiple solutions when the value of λ is small using very few collocation points. However to increase their accuracy would require many more collocation points and would no longer make these "simple" methods to implement. It is worthwhile to note that the Mickens discretization method performs as well as the nonlinear shooting method, and is also very easy to implement.

6 Conclusion

The goal of this paper has been to demonstrate the versatility of Mickens finite differences through the application of these nonstandard methods to singular linear boundary value problems, singular nonlinear boundary value problems with bifurcations and a nonsingular, nonlinear boundary value problem with bifurcations. In Section 3 the singular nature of the solution is much better captured near r equals zero by the numerical solution generated by the MFD compared to standard finite differences. In Section 4 the MFD is able to generate a numerical solution at exactly the same critical value of the nonlinear eigenvalue where the standard finite difference solution fails to converge. In Section 5 the MFD produces numerical solutions more accurate than the solution produced by standard finite differences and with less work than solutions generated by two different pseudospectral methods. The overall conclusion of this paper is that Mickens finite differences in general should be considered for use as a solution technique for a wide variety of problems. In particular, when the problem involves approximating derivatives in cylindrical or spherical coordinates, Buckmire's MFD scheme should be used.

Future work shall involve application of MFD to the "other" Bratu-Gel'fand problem, i.e. the classic Bratu problem in spherical coordinates. This problem has no known exact solution and posseses a much more complicated bifurcation curve [23]. It will be interesting to see whether MFD can be used to better resolve the limiting details of the bifurcation curve. In addition, there are other important nonlinear boundary value problems with and without bifurcations in cylindrical coordinates and spherical coordinates to which Buckmire's MFD scheme should be applied.

Acknowledgements

The author would like to thank Tom Witelski for first mentioning the name "Mickens" to me. The numerical calculations for this paper were performed using `Matlab` and `Mathematica` and the figures were all generated using `Matlab`.

References

[1] J. P. Abbott, "An efficient algorithm for the determination of certain bifurcation points" *Journal of Computational and Applied Mathematics* Volume **4** Number 1 (1978), 19-27.

[2] G. Adomian, *Solving Frontier Problems of Physics: The Decomposition Method* (Kluwer, Dordrecht, 1994).

[3] U. M. Ascher, R. M. M. Matheij and R. D. Russell, *Numerical Solution of Boundary Value Problems for Ordinary Differential Equations* (Society for Industrial and Applied Mathematics, Philadelphia, 1995).

[4] J. P. Boyd, "An analytical and numerical study of the two-dimensional Bratu equation," *Journal of Scientific Computing* Volume **1** Number 2 (1986), 183-206.

[5] G. Bratu, "Sur les équations intégrales non-linéaires," *Bulletins of the Mathematical Society of France* Volume **42** (1914), 113-142.

[6] R. Buckmire, *The Design of Shock-free Transonic Slender Bodies of Revolution* (Ph.D. thesis, Rensselaer Polytechnic Institute, Troy, 1994).

[7] R. Buckmire, "A new finite-difference scheme for singular boundary value problems in cylindrical or spherical coordinates" *Mathematics Is For Solving Problems* (Editors L. Pamela Cook and Victor Roytburd, Society for Industrial and Applied Mathematics, Philadelphia, 1996), 3-9.

[8] R. Buckmire, "On the design of shock-free transonic slender bodies of revolution," **AIAA Paper 98-2686** *American Institute of Aeronautics and Astronautics 2nd Theoretical Fluid Mechanics Meeting*, Albuquerque, 1998).

[9] R. Buckmire, "Investigations of nonstandard, Mickens-type, finite-difference schemes for singular boundary value problems in cylindrical or spherical coordinates," *Numerical Methods for Partial Differential Equations* Volume **19** Number 3 (2003), 380-398.

[10] R. Buckmire, "Application of a Mickens finite-difference scheme to the cylindrical Bratu-Gelfand problem," *Numerical Methods for Partial Differential Equations* Volume **20** Number 3 (2004), 327-337.

[11] S. Chandrasekhar, *An Introduction to the Study of Stellar Structure* (Dover Publications, New York, 1957).

[12] J. D. Cole and L. P. Cook, *Transonic Aerodynamics* (North-Holland, 1986).

[13] J. D. Cole and N. Malmuth, "Shock Wave Location on a Slender Transonic Body of Revolution," *Mechanics Research Communications* **16(6)** (1989), 353-357.

[14] J. D. Cole and A. F. Messiter. "Expansion Procedures and Similarity Laws for Transonic Flow," *Z.A.M.P.* **8** (1957), 1-25.

[15] J. D. Cole and E. M. Murman, "Calculation of Plane Steady Transonic Flows," *AIAA Journal* Volume **9** Number 1 (January 1971), 114-121.

[16] J. D. Cole, and D. W. Schwendeman, "Hodograph Design of Shock-free Transonic Slender Bodies," (*3rd International Conference on Hyperbolic Problems* Editors Bjorn Engqvist and Bertil Gustafsson, Uppsala, Sweden, June 11-15 1990).

[17] E. Deeba, S. A. Khuri and S. Xie, "An algorithm for solving boundary value problems," *Journal of Computational Physics* Volume **159** (2000), 125-138.

[18] B. A. Finlayson, *The Method of Weighted Residuals,* (Academic Press, New York, 1972).

[19] D. A. Frank-Kamenetski, *Diffusion and Heat Exchange in Chemical Kinetics,* (Princeton University Press, Princeton, 1955).

[20] I.M. Gelfand, "Some problems in the theory of quasi-linear equations," *Amer. Math. Soc. Transl. Ser. 2* Volume **29** (1963), 295-381.

[21] R. Haberman, *Elementary Applied Partial Differential Equations* (Prentice Hall, Englewood Cliffs, 1987).

[22] J. Jacobsen, and K. Schmitt,"The Liouville-Bratu-Gelfand problem for radial operators," *Journal of Differential Equations* **184** (2002), 283-298.

[23] D.D. Joseph, and T. S. Lundgren, "Quasilinear dirichlet problems driven by positive sources," *Archive for Rational Mechanics and Analysis* Volume **145** Number 10 (1998), 241-269.

[24] J. A. Krupp and E. M. Murman, "Computation of Transonic Flows past Lifting Airfoils and Slender Bodies," *AIAA Journal* Volume **10** Number 7 (July 1972), 880-886.

[25] J. Liouville, "Sur l'*é*quation aux diff*é*rences partielles $\frac{d^2 \log \lambda}{dudv} \pm \lambda 2a^2 = 0$, *J. Math. Pure Appl.*, **18** (1853), 71-72.

[26] J. S. McGough, "Numerical continuation and the Gelfand problem," *Applied Mathematics and Computation* Volume **89** (1998), 225-239.

[27] R. E. Mickens, "Difference equation models of differential equations having zero local truncation errors," *Differential Equations.*(Birmingham, Ala., 1983), 445-449, North-Holland Math. Stud., 92, (North-Holland, Amsterdam-New York, 1984).

[28] R. E. Mickens, "Exact solutions to difference equation models of Burgers' equation," *Numerical Methods for Partial Differential Equations* Volume **2** Issue 2 (1986), 123-129.

[29] R. E. Mickens, "Difference Equation Models of Differential Equations," *Mathematical and Computer Modelling* Volume **11** (1988), 528-530.

[30] R. E. Mickens, and A. Smith. "Finite-difference Models of Ordinary Differential Equations: Influence of Denominator Functions," *Journal of the Franklin Institute* **327** (1990), 143-145.

[31] R. E. Mickens, *Nonstandard Difference Models of Differential Equations* (World Scientific, Singapore, 1994).

[32] R. E. Mickens (editor), *Applications of Nonstandard Finite Differences*, (World Scientific, Singapore, 2000).

[33] R. E. Mickens, "Nonstandard Finite Difference Schemes for Differential Equations," *Journal of Difference Equations and Applications* Volume **8** Issue 9. (2002), 823-847.

[34] J. Ockendon, S. Howison, A. Lacey and A. Movchan, *Applied Partial Differential Equations,* (Oxford University Press, October 1999).

[35] D. L. Scharfetter, and H. K. Gummel, "Large-Signal Analysis of a Silicon Read Diode Oscillator," *IEEE Transactions on Electron Devices* Volume ED-16, Number 1, (January 1969), 64-84.

[36] K. Wanelik, "On the iterative solutions of some nonlinear eigenvalue problems," *Journal of Mathematical Physics* **30** Number 8 (August 1989), 1707-12.